Supporting Information

Spin Frustration in Antiperovskite Systems: ($TTF^{\bullet+}$ or $TSF^{\bullet+}$)$_3$[$(Mo_6X_{14})^{2-}Y^-$]

Takaaki Hiramatsu,*[a] Yukihiro Yoshida,[a] Gunzi Saito,*[a,b] Akihiro Otsuka,[c] Hideki Yamochi,[c] Yasuhiro Shimizu,[d] Yuma Hattori,[e] Yuto Nakamura, [e] Hideo Kishida,[e] Hiroshi Ito,[e] Kaplan Kirakci,[f] ‡ Stéphane Cordier,[f] and Christiane Perrin[f]

[a] *Faculty of Agriculture, Meijo University, 1-501 Shiogamaguchi, Tempaku-ku, Nagoya 468-8502, Japan*
[b] *Toyota Physical and Chemical Research Institute, 41-1, Yokomichi, Nagakute, Aichi 480-1192, Japan*
[c] *Research Center for Low Temperature and Materials Sciences, Kyoto University, Sakyo-ku, Kyoto 606-8501, Japan*
[d] *Department of Physics, Graduate School of Science, Nagoya University, Chikusa-ku Nagoya 464-8602, Japan*
[e] *Department of Applied Physics, Nagoya University, Chikusa-ku, Nagoya 464-8603, Japan*
[f] *Institut des Sciences Chimiques de Rennes, UMR CNRS 6226, Université de Rennes 1, Avenue du Général Leclerc, 35042 Rennes cedex, France*

Present address ‡ *Institute of Inorganic Chemistry of the Academy of Sciences of the Czech Republic*
Corresponding authors Takaaki Hiramatsu; *E-mail:* htakaaki@meijo-u.ac.jp
Gunzi Saito; *E-mail:* gsaito@meijo-u.ac.jp

Table S1. Crystal data and structure refinement of **1**

	1		
Chemical formula	$C_{18}H_{12}Cl_{15}Mo_6Se_{12}$		
Molecular weight	2283.19		
Temperature / K	300	100	25
Crystal dimensions / mm^3	0.17 × 0.15 × 0.08	0.17 × 0.15 × 0.08	0.12 × 0.10 × 0.06
Crystal system	Rhombohedral	Rhombohedral	Rhombohedral †
Space group	$R\bar{3}$	$R\bar{3}$	$R\bar{3}$ †
a / Å	10.9080(7)	10.8505(5)	10.8471(9) †
α / °	102.3484(3)	102.6318(2)	102.732(6) †
V / $Å^3$	1191.8(1)	1167.76(9)	1164.7(5) †
Z	1	1	1 †
D_{calc} / g cm^{-3}	3.181	3.247	3.255
Diffractometer	Bruker APEXII CCD area detector	Bruker APEXII CCD area detector	Rigaku Mercury CCD
Radiation type	MoKα	MoKα	MoKα
Absorption correction	Numerical	Numerical	Numerical
μ / mm^{-1}	11.554	11.792	11.823
No. of reflections measured	6674	6491	12352
No. of independent reflections	1797	1762	1779
R_{int}	0.0163	0.0143	0.0497
No. of parameters	78	78	78
Final R_1 values ($I > 2\sigma(I)$)	0.0180	0.0132	0.0151
Final $wR(F^2)$ values ($I > 2\sigma(I)$)	0.0343	0.0295	0.0325
Final R_1 values (all data)	0.0239	0.0145	0.0168
Final $wR(F^2)$ values (all data)	0.0363	0.0299	0.0325
Goodness of fit of F^2	1.094	1.086	1.043
Largest diff. peak / $eÅ^{-3}$	0.566	0.563	0.811
Largest diff. hole / $eÅ^{-3}$	−0.477	−0.419	−0.641
CCDC number	999368	999367	999366

(†) The values were evaluated by transformation from the hexagonal setting to rhombohedral setting, as data processing and structure analyses were conducted with the hexagonal setting.

Table S2. Crystal data and structure refinement of **2**

	2		
Chemical formula	$C_{18}H_{12}Br_{15}Mo_6Se_{12}$		
Molecular weight	2950.09		
Temperature / K	298	100	25
Crystal dimensions / mm^3	0.13 × 0.10 × 0.05	0.13 × 0.10 × 0.05	0.13 × 0.10 × 0.05
Crystal system	Rhombohedral	Rhombohedral	Rhombohedral †
Space group	$R\bar{3}$	$R\bar{3}$	$R\bar{3}$ †
a / Å	11.1579(5)	11.0988(9)	11.090(1) †
α / °	101.800(1)	102.0577(4)	102.147(8) †
V / $Å^3$	1286.3(1)	1261.1(2)	1259.7(7) †
Z	1	1	1 †
D_{calc} / g cm^{-3}	3.808	3.884	3.889
Diffractometer	Bruker APEXII CCD area detector	Bruker APEXII CCD area detector	Rigaku Mercury CCD
Radiation type	MoKα	MoKα	MoKα
Absorption correction	Numerical	Numerical	Numerical
μ / mm^{-1}	21.576	22.007	22.032
No. of reflections measured	7248	7072	13558
No. of independent reflections	1939	1903	1931
R_{int}	0.0228	0.0195	0.0541
No. of parameters	78	78	78
Final R_1 values ($I > 2\sigma(I)$)	0.0252	0.0203	0.0322
Final $wR(F^2)$ values ($I > 2\sigma(I)$)	0.0454	0.0395	0.0669
Final R_1 values (all data)	0.0382	0.0258	0.0354
Final $wR(F^2)$ values (all data)	0.0488	0.0409	0.0691
Goodness of fit of F^2	1.026	1.013	1.130
Largest diff. peak / $eÅ^{-3}$	0.582	0.536	1.530
Largest diff. hole / $eÅ^{-3}$	−0.426	−0.491	−1.201
CCDC number	999365	999364	999363

(†) The values were evaluated by transformation from the hexagonal setting to rhombohedral setting, as data processing and structure analyses were conducted with the hexagonal setting.

Table S3. Crystal data and structure refinement of $(TTF)_3[(Mo_6Br_{14})Br]$

	$(TTF)_3[(Mo_6Br_{14})Br]$	
Chemical formula	$C_{18}H_{12}Br_{15}Mo_6S_{12}$	
Molecular weight	2387.29	
Temperature / K	300	100
Crystal dimensions / mm^3	0.18 × 0.16 × 0.11	0.18 × 0.16 × 0.11
Crystal system	Rhombohedral	Rhombohedral
Space group	$R\bar{3}$	$R\bar{3}$
a / Å	10.9429(5)	10.8797(5)
α / °	100.915(1)	101.159(1)
V / $Å^3$	1228.5(1)	1203.4(1)
Z	1	1
D_{calc} / g cm^{-3}	3.227	3.294
Diffractometer	Bruker APEXII CCD area detector	Bruker APEXII CCD area detector
Radiation type	MoKα	MoKα
Absorption correction	Numerical	Numerical
μ / mm^{-1}	14.213	14.509
No. of reflections measured	6645	6614
No. of independent reflections	1835	1800
R_{int}	0.0260	0.0231
No. of parameters	78	78
Final R_1 values ($I > 2\sigma(I)$)	0.0276	0.0214
Final $wR(F^2)$ values ($I > 2\sigma(I)$)	0.0524	0.0459
Final R_1 values (all data)	0.0417	0.0259
Final $wR(F^2)$ values (all data)	0.0586	0.0476
Goodness of fit of F^2	1.066	1.033
Largest diff. peak / $eÅ^{-3}$	0.735	0.569
Largest diff. hole / $eÅ^{-3}$	−1.287	−1.971
CCDC number	999370	999369

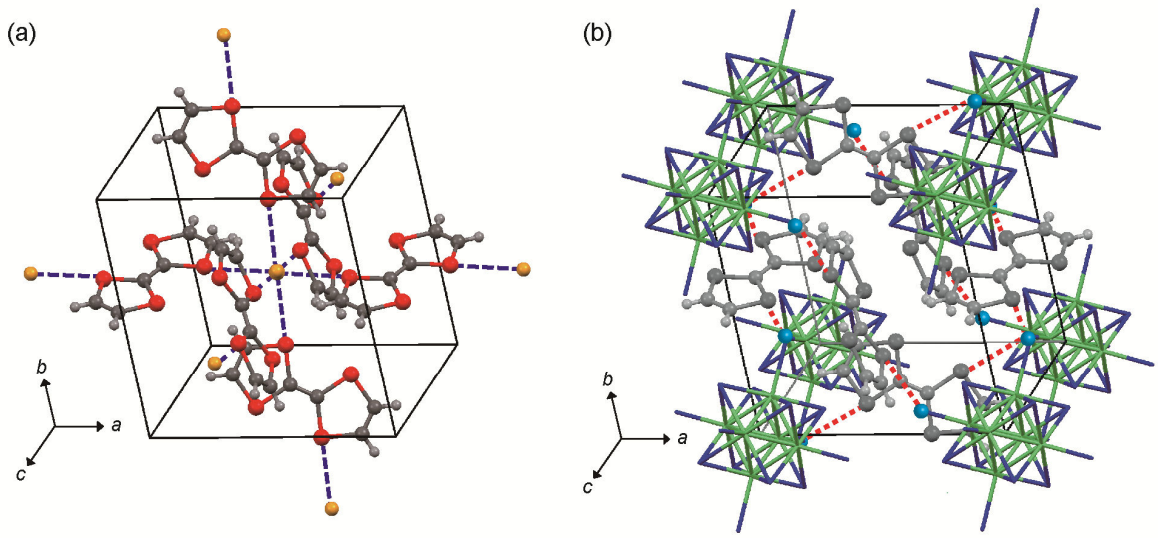

Fig S1. Short atomic contacts between chalcogen atoms in TTF or TSF and (a) halogen anion Y (dashed blue line) and (b) apical halogen X^a in the Mo cluster unit (dashed red line). Gray, dark gray, and orange balls represent hydrogen, carbon, and halogen Y atoms, respectively. Red balls are chalcogen atoms in TTF or TSF. (b) $[Mo_6X_{14}]$ cluster units are depicted in wire frame style (green and blue lines are molybdenum and halogen atoms, respectively). The apical halogens (X^a) in contact with TTF or TSF in the unit cell are depicted as cyan balls. TTF or TSF molecules are displayed in monochrome.

• Raman spectra of **2** and band assignment

To assign the observed Raman spectra, theoretical calculations were performed using Gaussian 98.[S1] Molecular geometry optimization and molecular orbital calculations of TSF^0 and TSF^{1+} molecules were carried out using the B3LYP functional with the 6-31G(d,p) basis set, enabling us to calculate normal vibrations. The calculated vibrational frequencies were scaled by a factor 0.9613.[S2] The normal vibration modes and these frequencies are summarized in Fig. S2 and Table S4, respectively.

Figure S3 shows the observed Raman spectrum of **2** at 10 K in the range from 200 to 1600 cm^{-1}. As the excitation laser (632.8 nm) is not resonant to the electronic transition band of $[Mo_6Br_{14}]^{2-}$ (absorption edge: 500 nm),[S3] all bands were not derived from $[Mo_6Br_{14}]^{2-}$,[S4] but from the TSF molecule (Fig. S9). Observed bands of TSF in **2** and reported bands of TSF^0[S5] are summarized in Table S4. Overall, good correspondence was seen for the fundamental modes of $a_g\nu_6$, $a_g\nu_5$, $a_g\nu_3$, and $a_g\nu_2$ between the observed spectrum of **2** and the calculated spectrum of TSF^{1+}; however, some differences were seen between 1300 and 1600 cm^{-1} (Fig. S4). The $a_g\nu_3$ mode was split in **2** (1395 and 1408 cm^{-1}), while no splitting was seen in the calculated spectrum (1373 cm^{-1}). This can be ascribed to the factor group splitting in the crystal; however, the origin of the band at 1465 cm^{-1} in **2** is currently unknown. The other bands in **2** observed in this range were interpreted by the overtone and combination modes of TSF^{1+}, as shown in Table S4. The charge sensitive bands ($a_g\nu_2$, $a_g\nu_3$) in the range of 1300 to 1600 cm^{-1} showed no significant temperature dependence from 300 to 10 K, as depicted in Fig. S5, indicating that the molecular charge of TSF in **2** did not change from 300 to 10 K.

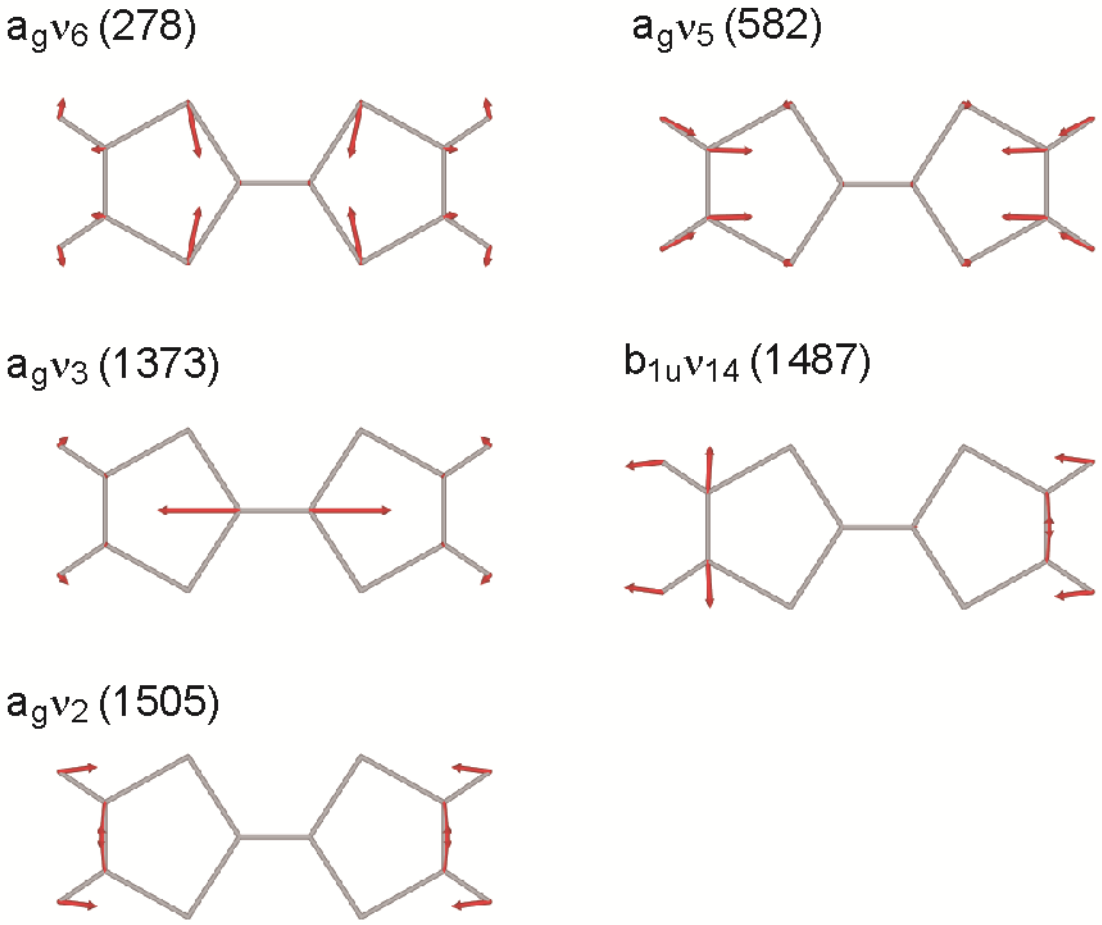

Fig. S2. Typical normal vibration modes of TSF^{1+}. The values in parentheses are the calculated wavenumbers of each mode.

Table S4. Calculated and observed Raman shifts (cm^{-1}) of TSF

	Observed		Calculated (B3LYP/6-31(d,p))		Evaluated Raman shift of overtone or combination mode from observed fundamental modes
Mode	TSF^{0}[S5]	TSF^{1+} (**2** ,10 K)	TSF^{0}	TSF^{1+}	TSF^{1+}
$a_g\nu_6$	272	289	273	278	–
$2 \times a_g\nu_6$	–	576	–	–	578(−2)
$a_g\nu_5$	599*	618	560	582	–
$3 \times a_g\nu_6$	–	865	–	–	867(−2)
$a_g\nu_5 + a_g\nu_6$	–	907	–	–	907(0)
$4 \times a_g\nu_6$	–	1151	–	–	1156(−5)
$a_g\nu_5 + 2 \times a_g\nu_6$	–	1191	–	–	1196(−5)
$a_g\nu_3$	1520	1395	1527	1373	Factor group splitting
		1408			Factor group splitting
$5 \times a_g\nu_6$	–	1440	–	–	1445(−5)
?	–	1465	–	–	–
$b_{1u}\nu_{14}$	–	–	1540	1487	–
$a_g\nu_5 + 3 \times a_g\nu_6$	–	1481	–	–	1485(−4)
$a_g\nu_2$	1549	1515	1553	1505	–

* Although the $a_g\nu_5$ mode of TSF^{0} was assigned to the band at 451 cm^{-1} in Ref. S5, we reassigned it to the band at 599 cm^{-1}, according to our calculation. The values in parentheses represent the difference between observed and evaluated Raman shift wavenumbers of overtone or combination modes.

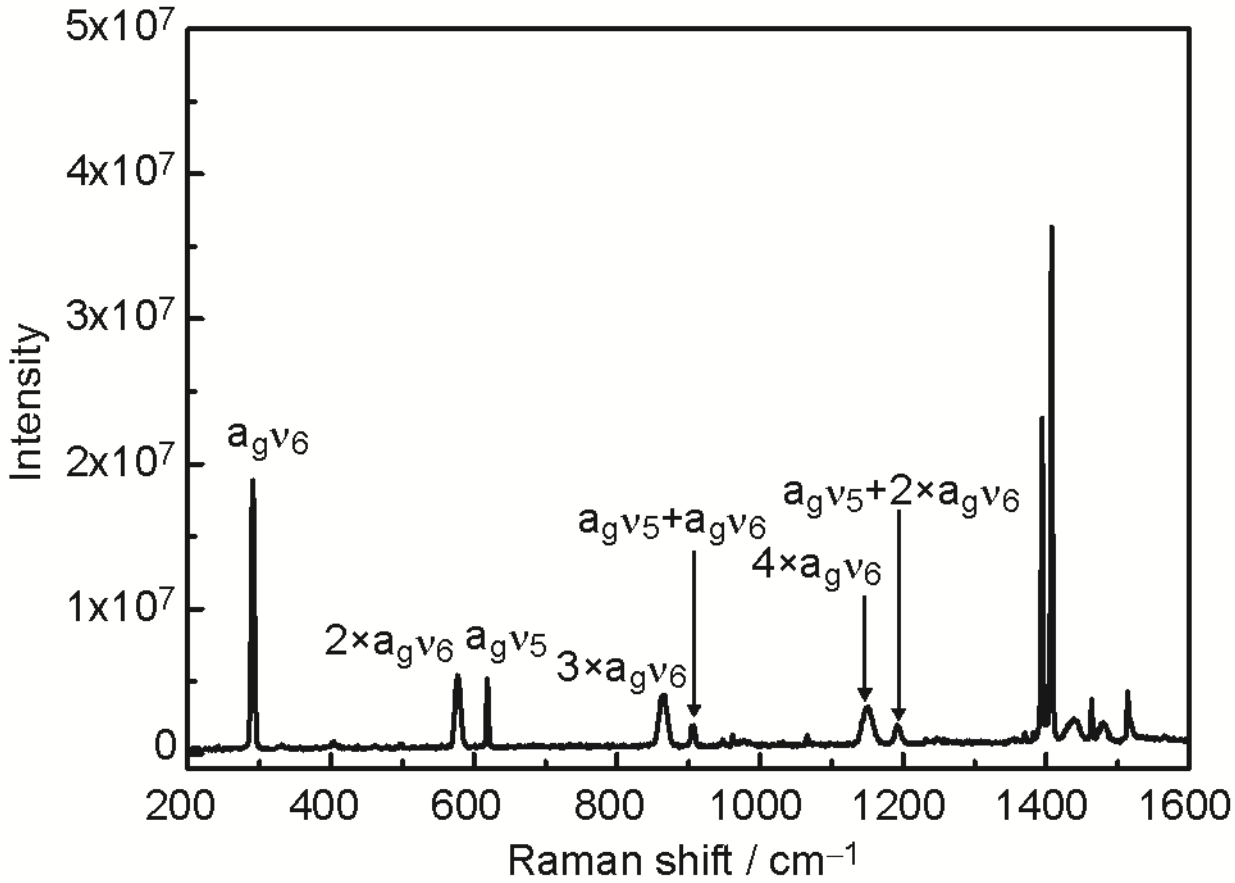

Fig. S3. Raman spectrum of **2** at 10 K.

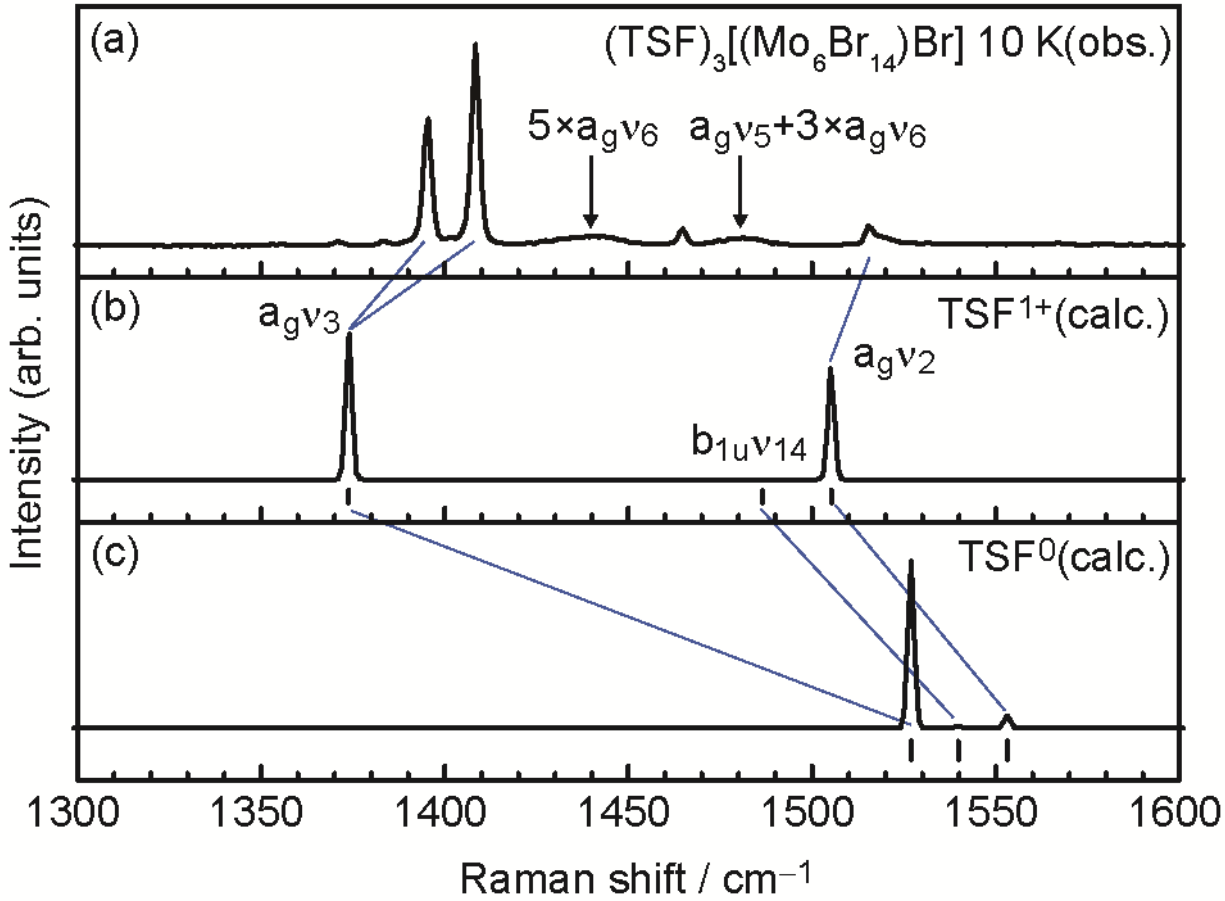

Fig. S4. (a) Raman spectrum of **2** and calculated Raman spectra of (b) TSF^{1+} and (c) TSF^{0}. In (b) and (c), the black vertical bars under the calculated spectra indicate the calculated wavenumber of the normal vibration modes. The blue lines indicate the assignment of each band. The calculated Raman shifts of TSF^{0} correspond well to the reported shifts (Table S4).[S5]

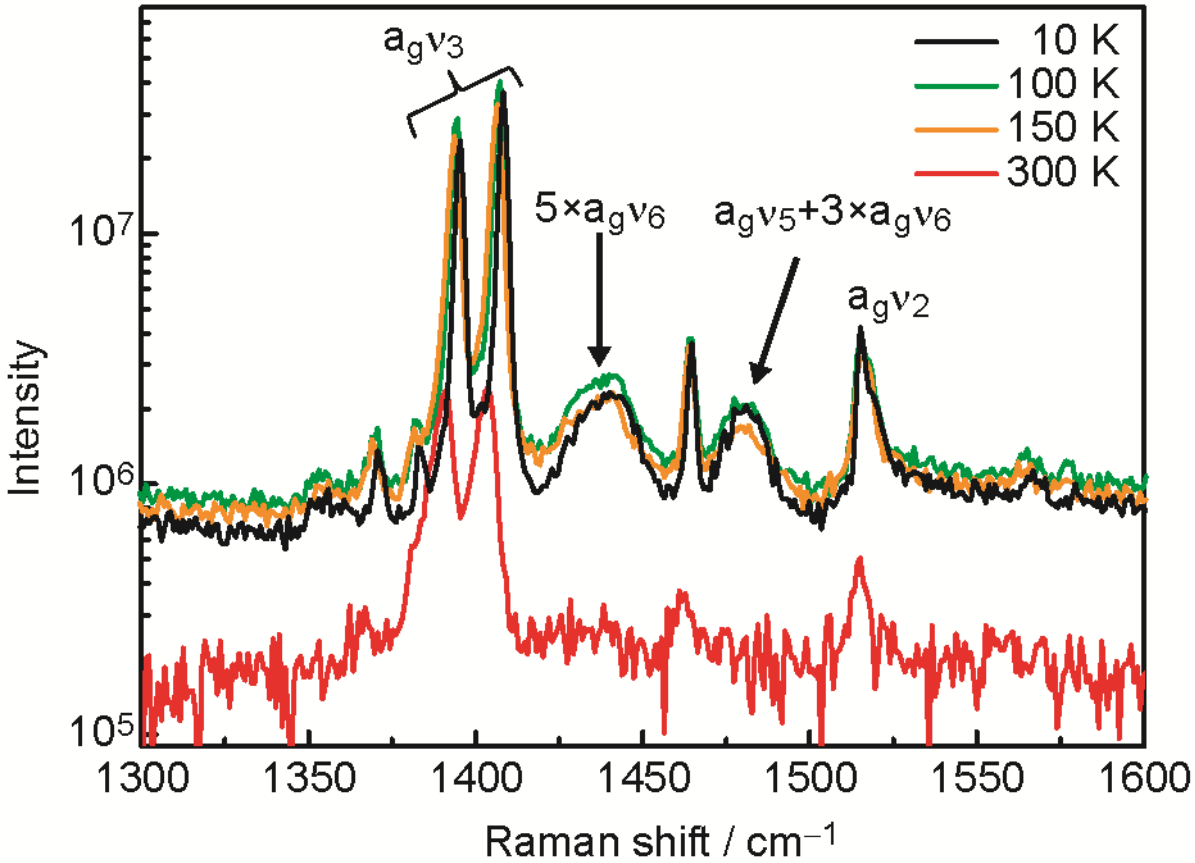

Fig. S5. Temperature dependence of the Raman spectra (300–10 K, 1300–1600 cm^{-1}). With the exception of the intensity of overtone and combination bands, the charge sensitive vibration modes ($a_g\nu_2$, $a_g\nu_3$) did not show any significant change between 300 and 10 K.

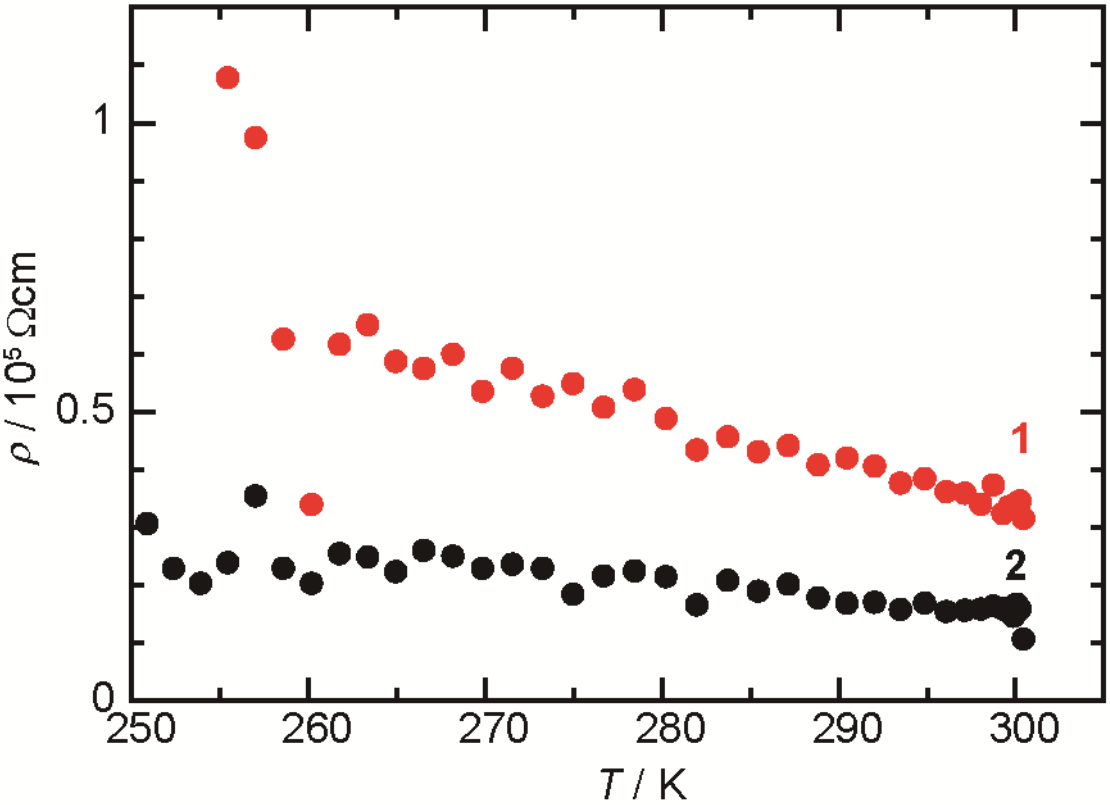

Fig S6. Temperature dependence of the resistivity of **1** (red circles) and **2** (black circles).

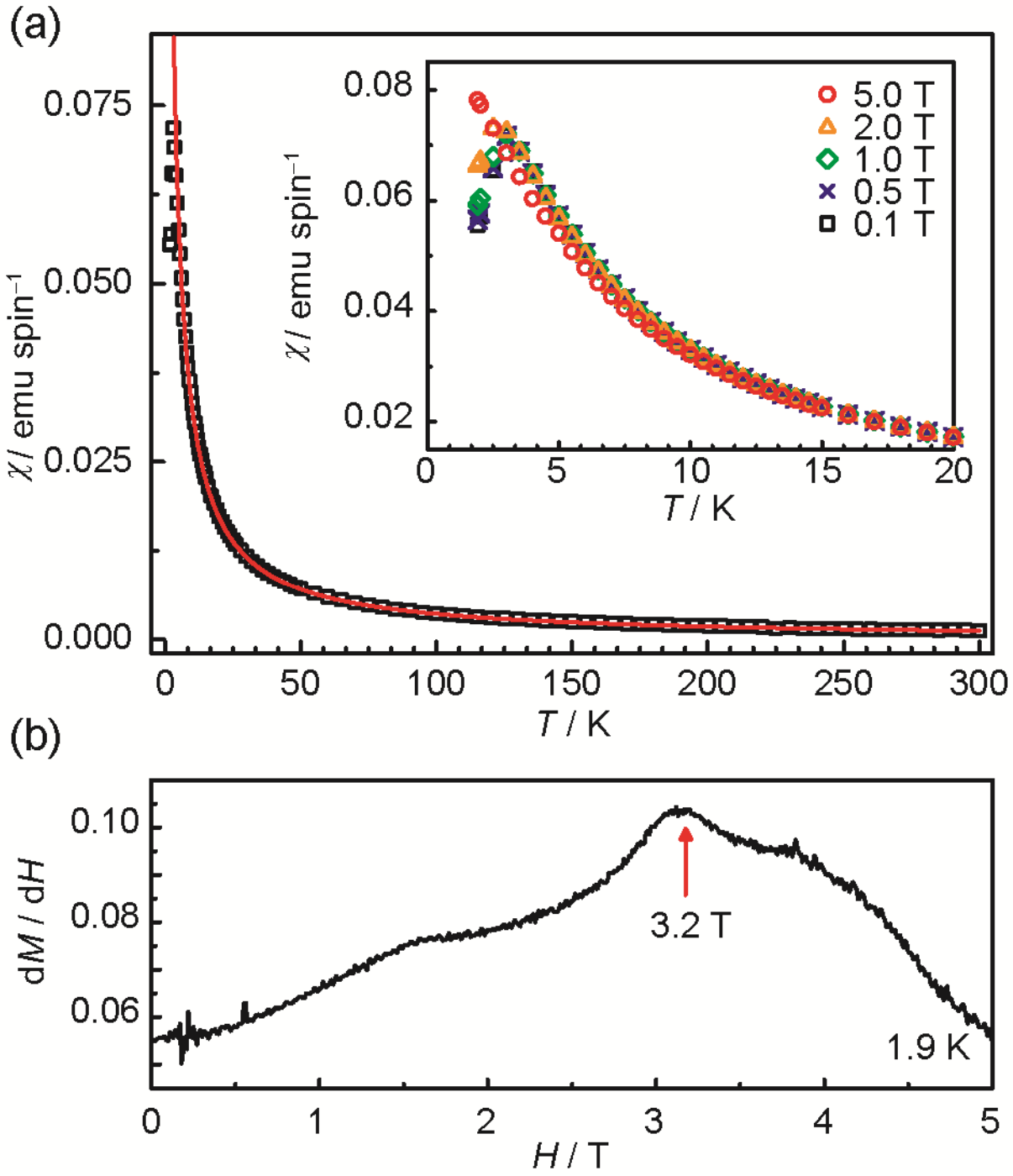

Fig S7. (a) Temperature dependence of the static magnetic susceptibility of **1** (polycrystals) at 0.1 T. Solid red line is the Curie-Weiss fit with C = 0.370 emu K mol^{-1} and Θ_{CW} = −1.6 K. Inset shows the magnetic field dependence (0.1–5.0 T) of χ below 20 K. (b) dM/dH at 1.9 K. A scatter of dM/dH at the region of H = 0.10–0.45 T resulted from inherent properties of the superconducting magnet. Red arrow indicates the spin-flop magnetic field.

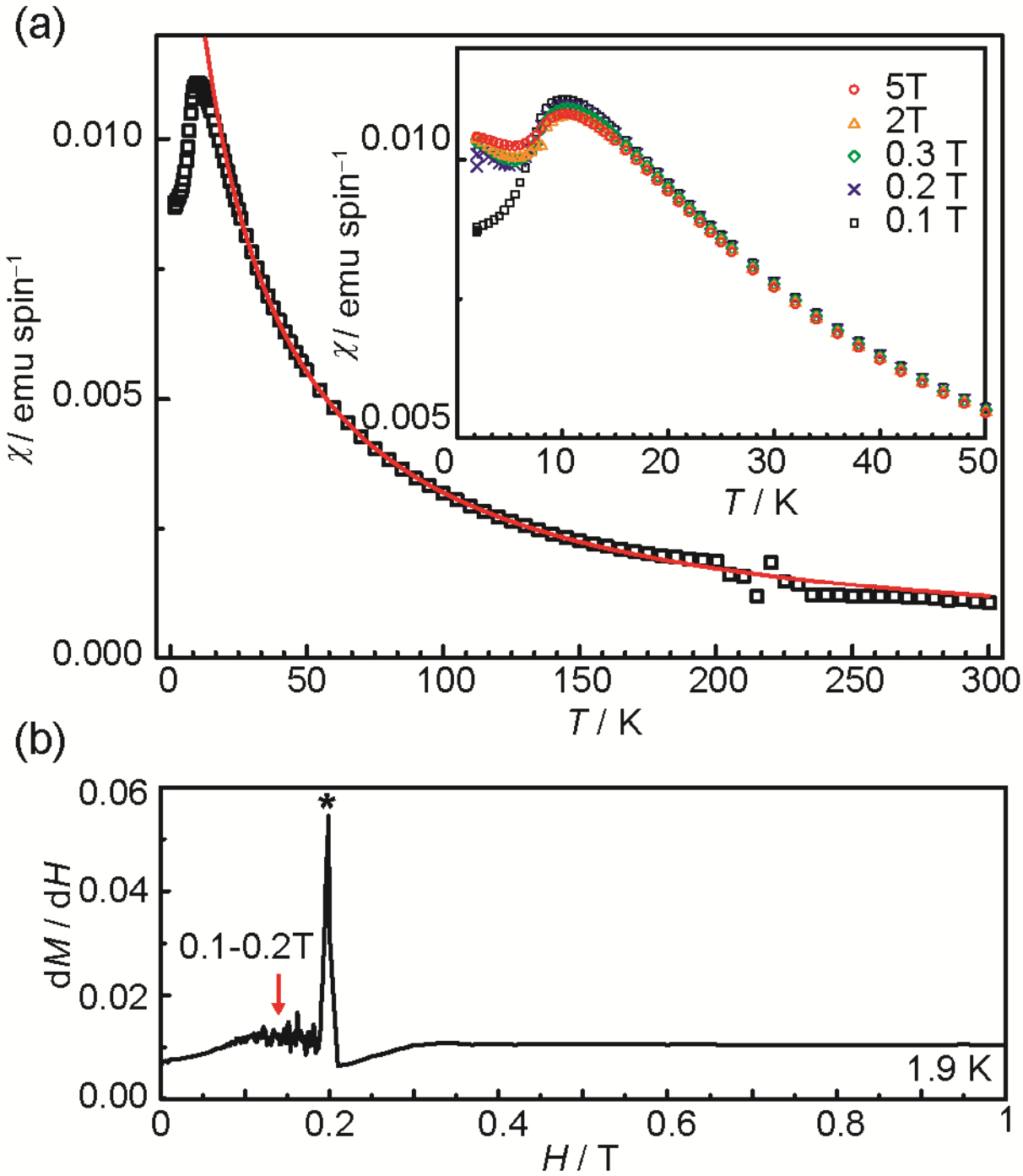

Fig S8. (a) Temperature dependence of the static magnetic susceptibility of $(TTF)_3[(Mo_6Br_{14})Br]$ (polycrystals) at 0.1 T. Solid red line is the Curie-Weiss fit with C = 0.381 emu K mol^{-1} and Θ_{CW} = −19.0 K. Inset shows the magnetic field dependence (0.1–5.0 T) of χ below 50 K. (b) dM/dH at 1.9 K. A scatter of dM/dH at the region of H = 0.10–0.45 T resulted from inherent properties of the superconducting magnet. The peak at 0.2 T indicated by * is also thought to the same origin; therefore, the spin flop magnetic field is deduced to be 0.1–0.2 T, as indicated by the red arrow.

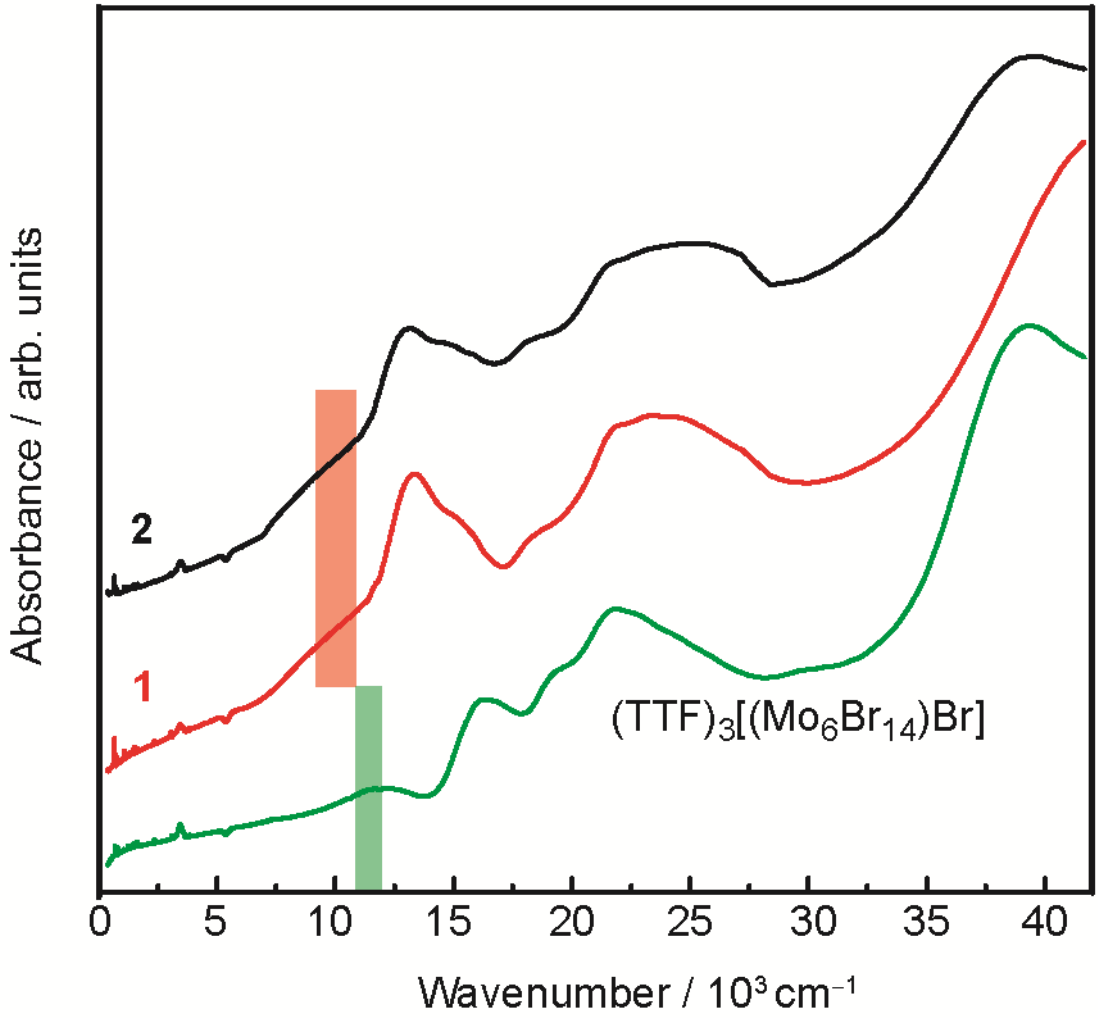

Fig S9. Optical absorption spectra of $(TTF)_3[(Mo_6Br_{14})Br]$ (green line), **1** (red line), and **2** (black line). The estimated peaks positions of the first CT absorption band are indicated by the red zone (1.2–1.4 eV) for **1** and **2** and the green zone (1.4–1.5 eV) for $(TTF)_3[(Mo_6Br_{14})Br]$.

References

S1. M. J. Frisch, G. W. Trucks, H. B. Schlegel, G. E. Scuseria, M. A. Robb, J. R. Cheeseman, V. G. Zakrzewski, J. A. Montgomery, Jr., R. E. Stratmann, J. C. Burant, S. Dapprich, J. M. Millam, A. D. Daniels, K. N. Kudin, M. C. Strain, O. Farkas, J. Tomasi, V. Barone, M. Cossi, R. Cammi, B. Mennucci, C. Pomelli, C. Adamo, S. Clifford, J. Ochterski, G. A. Petersson, P. Y. Ayala, Q. Cui, K. Morokuma, N. Rega, P. Salvador, J. J. Dannenberg, D. K. Malick, A. D. Rabuck, K. Raghavachari, J. B. Foresman, J. Cioslowski, J. V. Ortiz, A. G. Baboul, B. B. Stefanov, G. Liu, A. Liashenko, P. Piskorz, I. Komaromi, R. Gomperts, R. L. Martin, D. J. Fox, T. Keith, M. A. Al-Laham, C. Y. Peng, A. Nanayakkara, M. Challacombe, P. M. W. Gill, B. Johnson, W. Chen, M. W. Wong, J. L. Andres, C. Gonzalez, M. Head-Gordon, E. S. Replogle, J. A. Pople, Gaussian 98, Revision A.11.2, Gaussian, Inc., Pittsburgh PA, 2001.

S2. M. W. Wong, *Chem. Phys. Lett.*, 1996, **256**, 391-399.

S3. A. W. Maverick, J. S. Najdzionek, D. MacKenzie, D. G. Nocera, H. B. Gray, *J. Am. Chem. Soc.*, 1983, **105**,1878-1882.

S4. J. R. Schoonover, T. C. Zietlow, D. L. Clark, J. A. Heppert, M. H. Chisholm, H. B. Gray, A. P. Sattelberger, W. H. Woodruff, *Inorg. Chem.*, 1996, **35**, 6606-6613.

S5. K. Iwahana, H. Kuzmany, F. Wudl, E. A.-Shalom, *Mol. Cryst. Liq. Cryst.*, 1982, **79**, 39-47.